

Facile Process for the Fabrication of Durable Superhydrophobic Fabric with Oil/Water Separation Property

Mengnan Qu*, Lingang Hou, Jinmei He, Juan Feng, Shanshan Liu, and Yali Yao

College of Chemistry and Chemical Engineering, Xi'an University of Science and Technology, Xi'an 710054, China

(Received June 23, 2016; Revised October 16, 2016; Accepted October 22, 2016)

Abstract: A durable superhydrophobic fabric with oil/water separation property has been successfully prepared by introducing the modified silica nanoparticles and polysiloxane. The as-prepared fabric shows liquid repellency not only to water but also to coffee, milk and tea droplets, which are normal in daily life. Furthermore, the treated fabric shows simultaneous superhydrophobicity and superoleophilicity, which could be utilized as materials to separate oil/water mixture with high efficiency. It is important to note that the obtained fabric kept stable superhydrophobicity even after it suffered severe friction damage. The surface morphologies of untreated/treated fabrics were characterized by the scanning electron microscopy. The chemical compositions were characterized by X-ray photoelectric energy spectroscopy and Fourier transform infrared spectrum. This functionalized fabric will be helpful for developing superhydrophobic and selective oil adsorption materials.

Keywords: Superhydrophobic, Fabric, Nanoparticles, Oil/water separation, Durable

Introduction

Grid structure is welcomed in various fields because of its excellent characteristics (such as high strength, mechanically durable against wear or shear, etc.) [1,2]. The demands for different environments make it desirable to render multi-functional grid structure [3-5]. Currently, the superhydrophobicity, as one extreme case of wettability, has aroused a significant amount of research [6-10]. Waterproofing [11-14], superoleophobic [15], superamphiphobic [16,17] and antimicrobial efficacy [18] of fabric may be considered as potential applications for the superhydrophobic effect. Thus, the superhydrophobic grid structure, characterized by a high water contact angle of greater than 150° , has attracted worldwide attention for their potential market and economic benefits [19-24].

Superhydrophobicity of grid structure is attributed to cooperative effect of the low surface energy and the hierarchical micro/nano structure [25-27]. Heretofore, many researchers have been studied the fabrication of superhydrophobic grid structure and some relevant results have been reported [28-34]. For instance, Li and co-workers prepared a porous, superoleophilic and superhydrophobic miniature oil containment boom (MOCB) for the *in situ* separation and collection of oils from the surface of water [35]. Shiratori and co-workers fabricated a superhydrophobic polyester mesh by the progress of chemical etching and fluorosilane chemical vapor deposition, and the surface can also be used as an oil/water separation material because of its mesh structure [3]. Not only metal and polymer grid, but also functional fabrics and fibers have been reported in superhydrophobic. Abbas and co-workers reported a facile one step process by the incorporation of silica nanoparticles and hexadecyltrimethoxysilane *via* solution

immersion process to prepare superhydrophobic cotton fabric [36]. Xue and co-workers reported a simple method to prepare superhydrophobic poly(ethylene terephthalate) (PET) textile surfaces with self-cleaning property on PET textiles by chemical etching of the fiber surfaces and coating with polydimethylsiloxane [37]. Ou and co-workers aim to convert used cigarette filters to superhydrophobic fibers (SFs), which can be used for cleanup of oil spills on water [38]. Zhou and co-workers reported a single-step fabrication method for creating robust superhydrophobic cotton fabrics by *in situ* vapor phase deposition [39]. Superhydrophobic fabric will be widely used in daily life where fabric surfaces are exposed to the environment [17]. But one of the challenges faced by the existing superhydrophobic fabric is the durability. Most of the existing superhydrophobic surfaces lack of enough durability so that the fabrication of durable superhydrophobic surfaces is crucial [40].

Herein, we report a strategy to obtain durable superhydrophobic fabric by a two-step method. The first step is that the silica nanoparticles functionalized with methyltriethoxy silane (MTES) and their *in situ* incorporation onto fabric, which provided the fabric sufficient roughness and flexibility to obtain the superhydrophobic durability. The second step is the superhydrophobization with aluminate coupling agent (ACA) which bestows the superhydrophobicity to the fabric. ACA was adopted here as modifier, which is a kind of low-cost and environment-friendly reagent. To the best of our knowledge, ACA is rarely adopted to the preparation of the durable superhydrophobic fabric with oil/water separation property. The as-prepared fabric shows liquid repellency not only to water but also to coffee, milk and tea droplets, which are normal in daily life. Furthermore, the treated fabric shows simultaneous superhydrophobicity and superoleophilicity, which could be utilized as the materials to separate oil/water mixture with high efficiency. It is important to note that the

*Corresponding author: mnanqu@gmail.com

obtained fabric kept stable superhydrophobicity even after it suffered severe friction damage.

Experimental

Tetraethylorthosilicate (TEOS) was purchased from Tianjin Fuchen Chemical Reagent Co., Ltd. MTES was purchased from J&K Chemical Ltd. Aluminate coupling agent was purchased from Nanjing Daoning Chemical Co., Ltd. Anhydrous ethanol and ammonia were purchased from Guangzhou Jinhua Chemical Reagent Co., Ltd. The raw fabrics were obtained from a garment factory in Xi'an. The obtained fabric was sequentially cleaned with distilled water and ethanol to remove the impurities, and dried at room temperature. All of these chemicals were used as received.

The silica nanoparticles functionalized with MTES (M-SiO₂) were prepared by modified Stöber method. Briefly, TEOS (5 ml) and MTES (3 ml) were successively added dropwise to a round-bottom flask containing 25 ml of anhydrous ethanol under the condition of magnetic stirring. Then, a piece of cleaned fabric was immersed in the resultant solution. 20 ml of ammonia was added as the catalyst, and stirred for 5 minutes. Subsequently, the reaction was conducted by ultrasonic dispersed for 90 minutes. The treated fabric was removed from the solution and thoroughly rinsed in anhydrous ethanol to get rid of residual materials. Dried at 120 °C for 1 h, and noted as M-SiO₂ fabric.

The fabric was superhydrophobization by aluminate coupling agent. 0.5 g aluminate coupling agent was added under magnetic stirring to round-bottomed flask containing 15 ml ethanol, and ultrasonic dispersion for 20 minutes after fully dissolved. The flask was transferred into a preheated water bath that was heated at a constant temperature of 70 °C. Then, the pre-treated fabric was soaked into the flask for 6 hours. Finally, the fabric was removed from the solution, and dried at 120 °C for 2 h.

Static contact angle measurements were carried out using an optical contact angle goniometer (JC2000DM, China) and the average of five readings was used as the final contact angle of each sample. The surface morphologies of the fabric were investigated by a scanning electron microscopy (SEM, JEOL JSM-6460LV). All the samples were coated with gold cluster before the SEM investigation. Infrared

spectra were recorded using FTIR-spectrophotometer (Perkin Elmer FTIR System 2000). Samples were cut into very small pieces and then grounded and compressed with KBr salt into a thin pellet to form KBr disc. Different spectra were collected over the range of 500-4000 cm⁻¹. The surface chemical compositions were investigated by an X-ray photoelectron spectroscopy (XPS, K-Alpha, USA). The superhydrophobic durability test of treated fabrics was evaluated by sandpaper. The fabric was repeatedly rubbed with sandpaper until it was broken, and then the static contact angles of the broken fabric were measured. To investigate the long time superhydrophobic stability, the modified fabric was exposed to the natural environment for 7 days and then water droplets impact experiment was carried out. In the progress of water droplets impact, water droplets of 50 μl, which could impinge the fabric surface with a velocity up to v=3 m/s. After impinging by 5000 water droplets, the WCA was measured.

Results and Discussion

As shown in Figure 1, the silica nanoparticles functionalized with MTES were initially prepared from a modified Stöber procedure. The SiO₂ particles were *in situ* formed and the METS was also polymerized on the surface of fabrics. The MTES was used to embed and fix the SiO₂ particles in the spacing of the fabric fibers. It was used also to render the M-SiO₂ appropriate flexibility. The *in situ* formed M-SiO₂ fabricated the micro/nano scale roughness structures of the fabric. And the fabric showed hydrophobicity with a water contact angle of 138°. Followed by superhydrophobization with ACA and then the superhydrophobic fabric was obtained. It was found that the WCA remained at 154°. ACA is an important and environment-friendly surfactant. As cross-linker, aluminate coupling agent has two important roles in this study: stabilizing the obtained micro/nano scale roughness structure and making the fabric with superhydrophobicity by grafting the hydrophobic functional groups. There are two different kinds of functional groups in ACA, in which (RO)_x are hydrophilic and (OCR')_m are hydrophobic [41]. The hydrophilic groups can set off chemical reactions with the polar groups of the fabric and silica nanoparticles, making the fabric bonded with hydrophobic groups, the

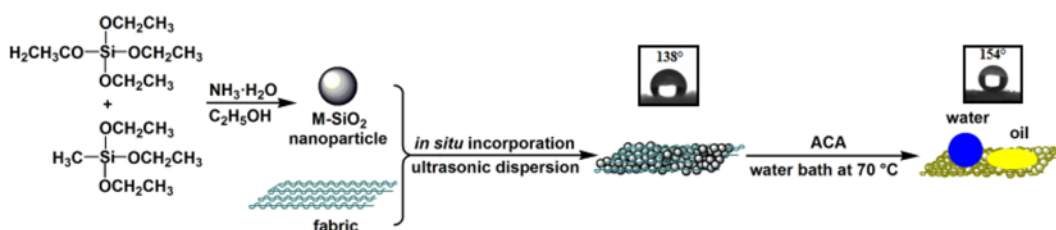


Figure 1. Schematic illustration of the fabrication process for superhydrophobic fabric. The M-SiO₂ nanoparticles were *in situ* formed on the surface of fabric with the subsequent modification of ACA.

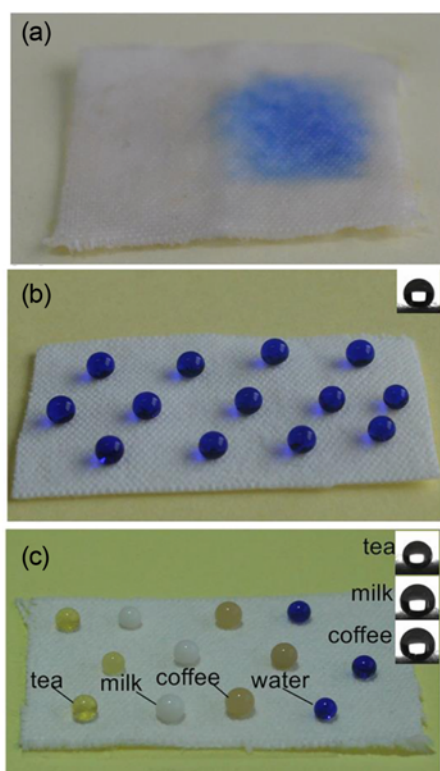


Figure 2. (a) Photograph of blue-colored water, tea, milk, and coffee droplets on the pristine fabric. These droplets have been absorbed by the fabric instantly. (b) Blue-colored water on the treated fabric. (c) Tea, milk, coffee and blue-colored water, on the treated fabric. Insets: (b) Profile of water droplet on the treated fabric. (c) Profiles of coffee milk and tea droplets on the treated fabric, respectively.

contact angle increases by grafting the hydrophobic functional groups to the surface of silica nanoparticles, which can reduce the surface energy greatly. And the durability improved by stabilizing the obtained micro/nano scale roughness structure.

Wettability examination was showed by water contact angle and photographs of the common household liquid droplets deposited on the surface of fabrics [36], as shown in Figure 2. For the pristine fabric, when common household liquid droplets were dropped on it, no contact angle could be measured due to the complete absorption of droplets into the fabric (Figure 2(a)). After the fabric was rendered superhydrophobic by modification with M-SiO₂ and ACA, all the droplets showed the spherical shape and the contact angle of water reach to 154° for a 10 μl droplet, as shown in Figure 2(b) and 2(c). The contact angles of tea, milk and coffee droplets on the fabric surface are 154°, 152° and 150°, respectively. This indicates that the sufficient micro/nano roughness of M-SiO₂ nanoparticles combined with the low surface energy of ACA have made significant contributions to the liquid repellency of the fabric.

Durability and stability are very important for the practical

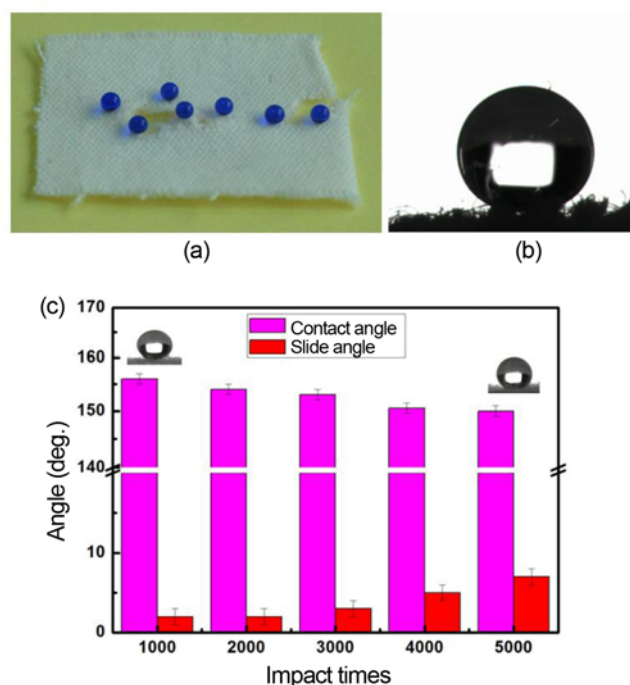


Figure 3. (a) Photograph of a water droplet on the broken area of treated fabric after abrasion with sandpaper, (b) optical images of water droplet sitting on the broken area of treated fabric, and (c) exposed to the natural environment for 7 days and then the change of hydrophobicity of the fabric after water droplets impact.

application of superhydrophobic fabric [39]. According to the formation mechanism of this superhydrophobic fabric, there are covalent bonds formed within M-SiO₂ and between M-SiO₂ and the substrate, which endow the obtained fabric with the durability required for severe abrasion. In this work, abrasion with sandpaper was employed to test the superhydrophobic durability of the fabric. As seen from Figure 3(a), the treated fabric retained its superhydrophobicity even after suffered severe friction damage. Water contact angle could still attain 153° in the area which suffered destruction (Figure 3(b)). To investigate the long time superhydrophobic stability, the modified fabric was exposed to the natural environment for 7 days and then water droplets impact experiment was carried out, which can observe the change of hydrophobicity of the fabric after testing for the long time superhydrophobic stability more clearly from Figure 3(c). After impinging by 5000 water droplets, the fabric was still superhydrophobic with a CA of 150°. After the treatments as mentioned above, the long time superhydrophobic stability of the fabric was demonstrated.

Figure 4 provides the morphological information of the fabric before and after the treatment. The pristine cotton fabric displays fiber bundles (Figure 4(a)), and the individual fiber presents a smooth longitudinal fibril structure (Figure 4(b)). As shown in Figure 1, the superhydrophobic fabric was obtained from a two-step procedure. The first step is the

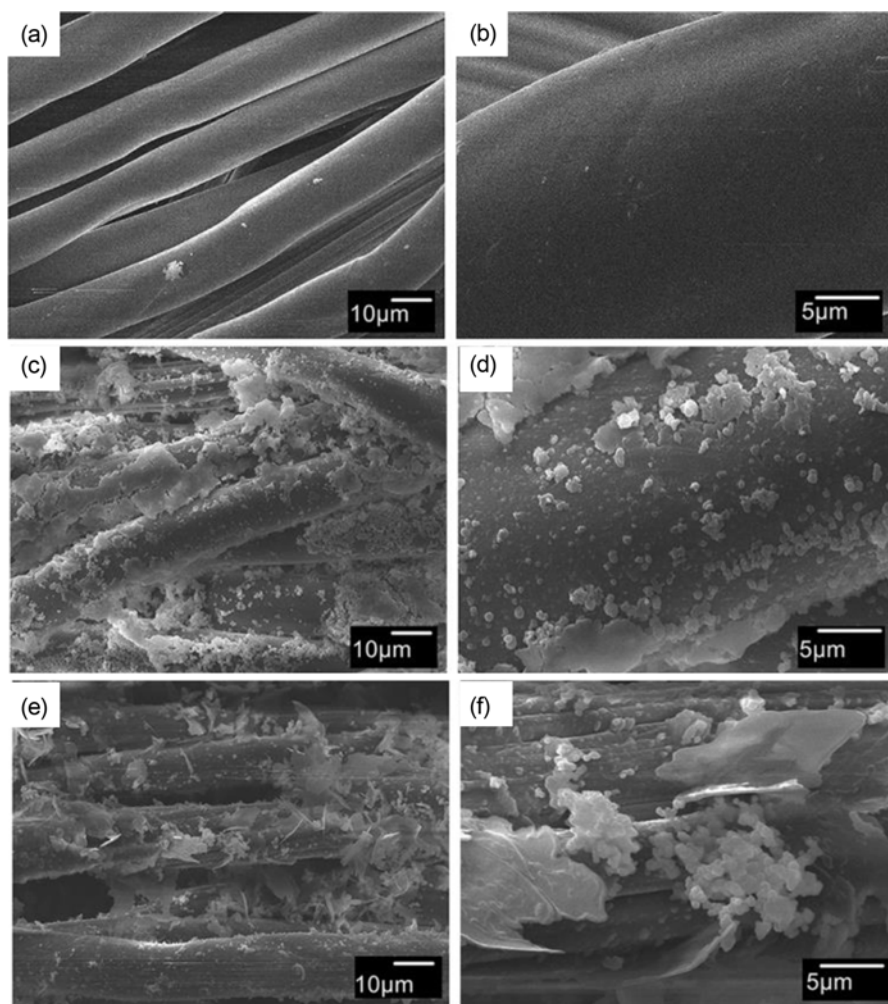


Figure 4. SEM images at different magnifications of (a, b) pristine fabric, (c, d) the fabric after one step treatment with M-SiO₂, and (e, f) the fabric after two steps treatment with ACA, respectively.

incorporation of the silica nanoparticles and polysiloxane *in situ* formed on the surface of fabrics. After this treatment, it is obvious that the silica nanoparticles and the polysiloxane were random and close-packed distributed throughout the fiber surface (Figure 4(c) and 4(d)). This step provided a degree of roughness to the surface of fiber and imparted nanoscale surface roughness. Then, M-SiO₂ and the fabric were further modified with ACA to lower its surface energy. After treated with ACA, obvious morphology changes have occurred and it can be observed from the Figure 4(e) and 4(f). The changes were properly caused by the modification and adhesions of ACA on fabric surface. This result demonstrates the superhydrophobicity obtained by synergism of the surface roughness and low surface energy.

To examine surface chemical composition of the fabric, XPS measurement was used to further investigate the elements of the fabric [20,24]. For the untreated fabric, only peaks corresponding to C and O were observed (Figure

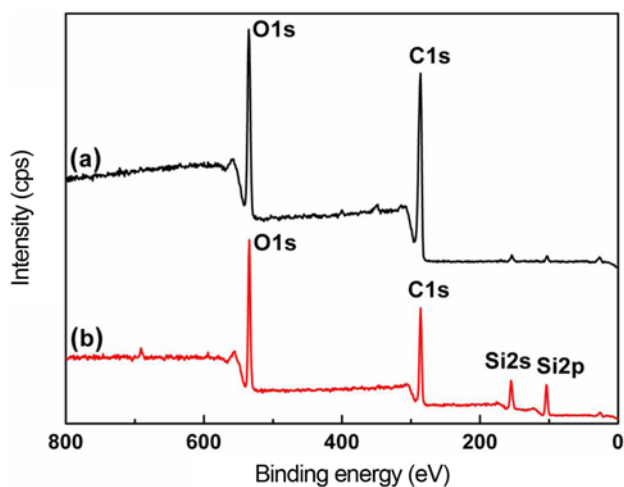


Figure 5. XPS survey spectra of (a) the pristine fabric and (b) the treated fabric.

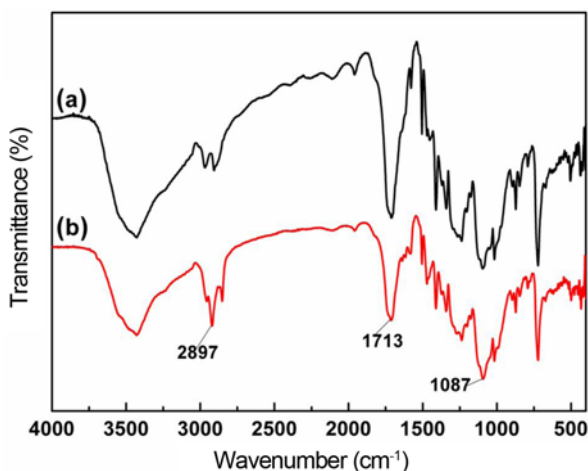


Figure 6. FT-IR spectra of (a) the pristine fabric and (b) the M-SiO₂ treated fabric.

5(a)). After being treated by M-SiO₂, there were new peaks appeared (Figure 5(b)) at 153.2 and 102.4 eV, which are attributed to Si 2s, and Si 2p signals, respectively. The characteristic peaks of Si 2s and Si 2p manifested that the presence of Si element on the surface of the fabric was evident. That is to say, the siloxane segments had successful covered the external surface of the fabric.

To further corroborate the modified silica particles which had been successfully *in situ* formed on the surface of fabrics, FTIR spectroscopy was used to characterize the pristine and treated fabrics [17,23,32]. The FTIR spectra of both spectrums showed characteristic bands of fabrics. Such as the broad band at around 3500 cm⁻¹ was attributed to hydroxyl group. The adsorption bands at around 2800-2900 cm⁻¹ were attributed to -CH stretching vibrations. The -OH bending at 1713 cm⁻¹ indicated adsorbed molecular water in the fabric (Figure 6(a) and 6(b)). However, the FTIR spectrum of fabrics treated with M-SiO₂ showed new band at 2897 cm⁻¹ (Figure 6(b)) corresponding to the stretching vibration of the -CH₃ group, which demonstrated that the long chain hydrocarbon of MTES was indeed attached to the surface of the silica nanoparticles *via* chemical bonds. Furthermore, increased band intensity at the 1100-1000 cm⁻¹ region due to the typical absorption of the Si-O-Si bands of M-SiO₂ is overlapped by cellulose bands of C-O bending modes. In addition, significant reductions of the -OH bending band at around 1713 cm⁻¹ were observed, which confirms the moisture reduction of the treated fabric. These spectra thus confirm the successful *in situ* formed of M-SiO₂ from the surfaces of the fabric.

The effect of the MTES concentration on the hydrophobicity of the treated fabric was also investigated. A series of fabric that modified by M-SiO₂ were prepared by changing the MTES concentration from 1 % to 9 %. The hydrophobicity of the treated samples was shown in Figure 7. It can be seen

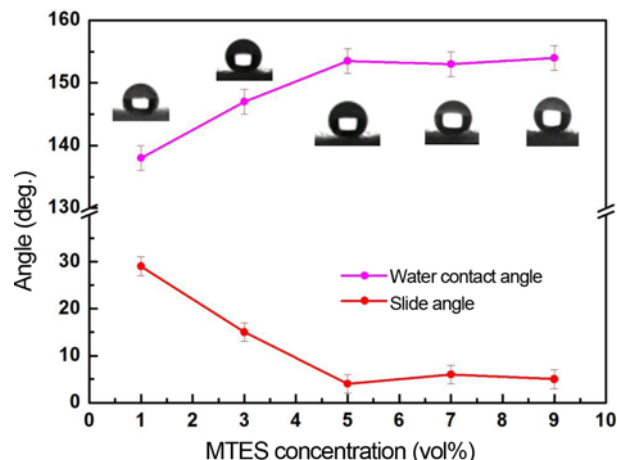


Figure 7. Effect of MTES concentration on the hydrophobicity of treated fabrics.

that with the increase of MTES concentration, the slide angle of the treated fabric decreased significantly, the water contact angle gradually increased. However, when the MTES concentration was more than 5 %, the hydrophobicity of treated fabrics had little change. When the MTES concentration was 5 %, the coated cotton fabric had a water contact angle of 153.5°. While the MTES concentration was 9 %, the coated cotton fabric had a water contact angle of 154°. Obviously, when MTES concentration was higher than 5 %, the hydrophobicity of the fabric didn't change almost. The explanation could be that the long chain hydrocarbon of MTES was attached to the surface of the silica nanoparticles *via* chemical bonds. With the MTES concentration increased, long chain hydrocarbon tended to enrich on the surface of silica nanoparticles. But too high concentration of MTES can't result the hydrophobicity of the treated fabric was improved anymore, which originates from the accumulation of SiO₂ nanoparticles and decreases the surface roughness.

More interesting, the treated fabric showed simultaneous superhydrophobicity and superoleophilicity. For practical application, it is an excellent candidate material for removal of oil from water [28]. Colleseed oil dyed with methyl red was poured into the bottle which contained water dyed with methyl blue to form a thin layer (Figure 8(a) and 8(b)), then the oil/water mixture was stirred and allowed to stand for 10 minutes. As shown in Figure 8(c)-(f), a piece of treated fabrics was sunk below the oil/water interface. It strongly repelled water and selectively adsorbed the oil when it touched the oil surface. After selectively adsorbed oil from oil/water mixture, a fresh water surface was left (Figure 8(g) and 8(h)).

The separation efficiency of the fabric was further investigated, for different oil-water mixtures, the oil content in water differs from one another significantly, because a large difference exists for the density and solubility between

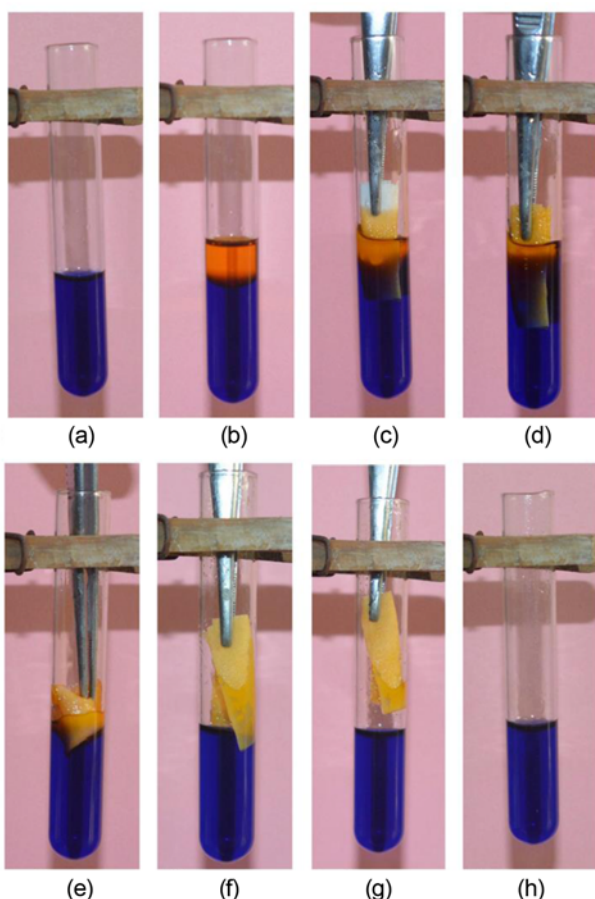


Figure 8. Photographs of (a) water dyed with methyl blue in a test tube, (b) colseeed oil dyed with methyl red was poured into the test tube, (c-f) the treated fabric was sunk below the oil/water interface, (g) removal of the treated fabric from oil/water mixture, and (h) water was left after the oil was selectively adsorbed.

oil and water. Thus the separation efficiency of fabric was given by the ratio of the weight of oil collected to that initially added to the mixture. Table 1 lists the separation efficiency of the fabric for different oil/water mixtures with their change of mass before and after separating the oil and water. And these values were a little bit higher than previously reported ones, for example, 96.5 % by Ou *et al.* [38]. Hence, the treated fabric could be utilized as materials to separate oil/water mixture with high efficiency.

It was very interesting to note that the treated fabric was

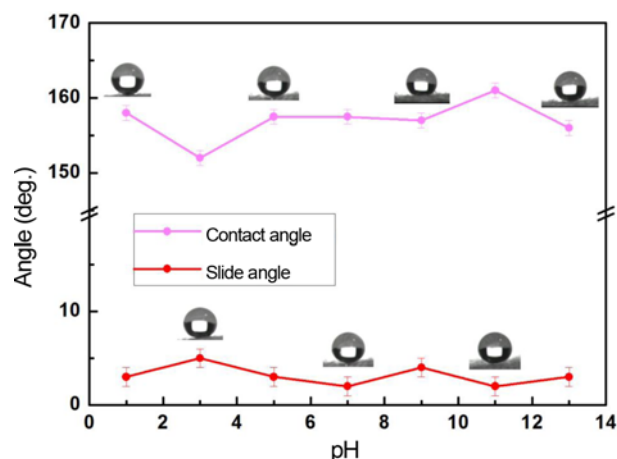


Figure 9. Contact angle and slide angle of different acidic and alkaline solutions on the surface of fabrics.

rinsed thoroughly by ethanol to get rid of the adsorbed oil and then dried in an oven at 120 °C. After drying, the fabric could be reused as before. After 50 cycles of rinsing and drying, the fabric still maintained the super repellency to water. Although the fabric lost the superhydrophobicity after 80 cycles, the WCA was still maintained at 143°. Not only pure water but also other different pH liquids as well, as showed in Figure 9, the modified fabric shows highly superhydrophobicity to a series of acidic and alkaline solutions which pH ranging from 1 to 13. These results imply a stable liquid repellency of as-prepared superhydrophobic fabric against normal daily life liquids, thus not only pure water but also other normal daily life liquids could be separated from the mixture.

Conclusion

In summary, by introducing the modified silica nanoparticles to fabric and then modified with ACA, a superhydrophobic fabric with durable and effective oil/water separation property has been prepared successfully. The effect of the MTES concentration on the hydrophobicity of the treated fabric was analyzed. With the increase of MTES concentration, the water contact angle of the treated fabric gradually increased. However, when MTES concentration was higher than 5 %, the hydrophobicity of the fabric didn't change almost. The as-prepared fabric showed liquid repellency to

Table 1. Separation efficiency of the fabric for different oil/water mixtures with their volume ratios of 1:1 and their change of mass before and after separating the oil and water

Oil/water mixtures (volume ratio=1:1)	Colseeed oil/water	Industrial white oil/water	Castor oil/water	Dichloromethane/water
Initial oil/water mixtures (g)	45.4176	45.6267	47.3779	55.4034
After separation (g)	23.9527	23.9428	24.2225	24.0007
Separation efficiency (η , wt %)	99.97	99.99	99.84	99.80

water, coffee, milk and tea droplets, which are all the household liquids. More interesting, the treated fabric showed simultaneous superhydrophobicity and superoleophilicity. It strongly repelled water and selectively adsorbed the oil when it touched the oil surface. For practical application, the treated fabric could be utilized as materials to separate oil/water mixture with high efficiency. More important, the obtained fabric kept stable superhydrophobicity even after it suffered severe friction damage.

Acknowledgment

The authors thank the National Natural Science Foundation of China (Grant No. 21473132, 21373158), the Shannxi Science and Technology Department (Grant No. 2014JM2047, 2013KJXX-41) for continuing financial support.

References

1. L. Wang, X. Zhang, B. Li, P. Sun, J. Yang, H. Xu, and Y. Liu, *ACS Appl. Mater. Interface*, **3**, 1277 (2011).
2. L. Xu, Z. Geng, J. He, and G. Zhou, *ACS Appl. Mater. Interface*, **6**, 9029 (2014).
3. N. Yokoi, K. Manabe, M. Tenjimabayashi, and S. Shiratori, *ACS Appl. Mater. Interface*, **7**, 4809 (2015).
4. T. Darmanin and F. Guittard, *Prog. Polym. Sci.*, **39**, 656 (2014).
5. X. Liu, Y. Xu, K. Ben, Z. Chen, Y. Wang, and Z. Guan, *Appl. Surf. Sci.*, **339**, 94 (2015).
6. B. Ge, X. Men, X. Zhu, and Z. Zhang, *J. Mater. Sci.*, **50**, 2365 (2015).
7. A. M. Al-Qutub, A. K. N. Saheb, N. Al-Aqeeli, and T. Laoui, *Sci. Adv. Mater.*, **4**, 1166 (2012).
8. C. H. Xue, S. T. Jia, J. Zhang, and L. Q. Tian, *Thin Solid Films*, **517**, 4593 (2009).
9. B. Deng, R. Cai, Y. Yu, H. Jiang, C. Wang, J. Li, L. Li, M. Yu, J. Li, L. Xie, Q. Huang, and C. Fan, *Adv. Mater.*, **22**, 5473 (2010).
10. Z. Guo, W. Liu, and B. L. Su, *J. Colloid Interf. Sci.*, **353**, 335 (2011).
11. E. Richard, R. V. Lakshmi, S. T. Aruna, and B. J. Basu, *Appl. Surf. Sci.*, **277**, 302 (2013).
12. B. Xu, Z. Cai, W. Wang, and F. Ge, *Surf. Coat. Technol.*, **204**, 1556 (2010).
13. G. Y. Bae, Y. Geun, B. G. Min, Y. G. Jeong, S. C. Lee, J. H. Jang, and G. H. Koo, *J. Colloid Interface Sci.*, **337**, 170 (2009).
14. J. P. Zhang, B. C. Li, L. Wu, and A. Q. Wang, *Chem. Commun.*, **49**, 11509 (2013).
15. B. Leng, Z. Shao, G. With, and W. Ming, *Langmuir*, **25**, 2456 (2009).
16. B. Xua, Y. Ding, S. Qu, and Z. Cai, *Appl. Surf. Sci.*, **356**, 951 (2015).
17. G. Zhang, S. Lin, L. Wyman, H. Zou, J. Hu, G. Liu, J. Wang, F. Li, F. Liu, and M. Hu, *ACS Appl. Mater. Interfaces*, **5**, 13466 (2013).
18. X. H. Ren, L. Kou, J. Liang, S. D. Woreley, Y. M. Tzou, and T. S. Huang, *Cellulose*, **15**, 593 (2008).
19. R. G. Karunakaran, C. Lu, Z. Zhang, and S. Yang, *Langmuir*, **27**, 4594 (2011).
20. B. T. Zhang, B. L. Liu, X. B. Deng, S. S. Cao, X. H. Hou, and H. L. Chen, *Colloid Polym. Sci.*, **286**, 453 (2008).
21. X. Bi and Z. Cai, *Appl. Surf. Sci.*, **254**, 5899 (2008).
22. T. Darmanin and F. Guittard, *J. Phys. Chem. C*, **118**, 26912 (2014).
23. C. Pereira, C. Alves, A. Monteiro, C. Magen, A. M. Pereira, A. Ibarra, M. R. Ibarra, P. B. Tavares, J. P. Araujo, G. Blanco, J. M. Pintado, A. P. Carvalho, J. Pires, M. F. R. Pereira, and C. Freire, *ACS Appl. Mater. Interfaces*, **3**, 2289 (2011).
24. H. F. Hoefnagels, D. Wu, G. With, and W. Ming, *Langmuir*, **23**, 13158 (2007).
25. C. X. Wang, T. J. Yao, J. Wu, C. Ma, Z. X. Fan, Z. Y. Wang, Y. R. Cheng, Q. Lin, and B. Yang, *ACS Appl. Mater. Interfaces*, **1**, 2613 (2009).
26. C. H. Xue, P. Zhang, J. Z. Ma, P. T. Ji, Y. R. Li, and S. T. Jia, *Chem. Commun.*, **49**, 3588 (2013).
27. H. J. Lee and J. R. Owens, *J. Mater. Sci.*, **45**, 3247 (2010).
28. X. Liu, L. Ge, W. Li, X. Wang, and F. Li, *ACS Appl. Mater. Interfaces*, **7**, 791 (2015).
29. Q. Zhu, Q. Gao, Y. Guo, C. Q. Yang, and L. Shen, *Ind. Eng. Chem. Res.*, **50**, 5881 (2011).
30. H. L. Zou, S. D. Lin, Y. Y. Tu, G. J. Liu, J. W. Hu, F. Li, L. Miao, G. W. Zhang, H. S. Luo, F. Liu, C. M. Hou, and M. L. Hu, *J. Mater. Chem. A*, **1**, 11246 (2013).
31. M. E. Yazdanshenas and M. Shateri-Khalilabad, *Ind. Eng. Chem. Res.*, **52**, 12846 (2013).
32. L. Hao, Q. An, and W. Xu, *Fiber. Polym.*, **13**, 1145 (2012).
33. H. Wang, H. Zhou, A. Gestos, J. Fang, and T. Lin, *ACS Appl. Mater. Interfaces*, **5**, 10221 (2013).
34. G. R. J. Artus, J. Zimmermann, F. A. Reifler, S. A. Brewer, and S. A. Seeger, *Appl. Surf. Sci.*, **258**, 3835 (2012).
35. F. Wang, S. Lei, M. Xue, J. Ou, and W. Li, *Langmuir*, **30**, 1281 (2014).
36. R. Abbas, M. A. Khereby, W. A. Sadik, and A. G. M. E. Demerdash, *Cellulose*, **22**, 887 (2015).
37. C. H. Xue, Y. R. Li, P. Zhang, J. Z. Ma, and S. T. Jia, *ACS Appl. Mater. Interfaces*, **6**, 10153 (2014).
38. J. Ou, B. Wan, F. Wang, M. Xue, H. Wu, and W. Li, *RSC Adv.*, **6**, 44469 (2016).
39. X. Zhou, Z. Zhang, X. Xu, F. Guo, X. Zhu, X. Men, and B. Ge, *ACS Appl. Mater. Interfaces*, **5**, 7208 (2013).
40. B. Wang, J. Li, G. Y. Wang, W. X. Liang, Y. B. Zhang, L. Shi, Z. G. Guo, and W. M. Liu, *ACS Appl. Mater. Interfaces*, **5**, 1827 (2013).
41. H. Li, M. N. Qu, Z. Sun, J. M. He, and A. N. Zhou, *J. Nanomater.*, **2013**, 497216 (2013).